Journal of Alloys and Compounds 509 (2011) 2311–2315

Contents lists available at ScienceDirect

Journal of Alloys and Compounds

journal homepage: www.elsevier.com/locate/jallcom

Effect of Ca substitution by Sr on the thermoelectric properties of $Ca_3Co_4O_9$ ceramics

F. Delorme*, C. Fernandez Martin, P. Marudhachalam, D. Ovono Ovono, G. Guzman

CORNING SAS, CETC, 7 Bis Avenue Valvins, 77210 Avon, France

ARTICLE INFO

Article history:
Received 30 September 2010
Received in revised form 25 October 2010
Accepted 28 October 2010
Available online 10 November 2010

Keywords:
Thermoelectric materials
Ceramics
Cobalt oxides
Substitution

ABSTRACT

$(Ca_{1-x}Sr_x)_3Co_4O_9$ polycrystalline samples (x = 0, 0.001, 0.002, 0.004, 0.005, 0.006, 0.01, 0.02, 0.1, 0.2, 0.3, 0.5 and 1) have been prepared by solid state reaction and sintered by spark plasma sintering. Their thermoelectric properties at high temperature have been studied (650–1000 K). The substitution limit is close to 20%. For higher Sr contents, a pseudo one-dimensional phase of the type $Sr_6Co_5O_{15}$ is appearing. The substitution of calcium by strontium does not significantly affect the Seebeck coefficient. Concerning electrical conductivity and power factor an optimum value exists for 0.5% substitution. Finally ZT values of samples with less than 20% Sr content are increased due to lower thermal conductivities. The dimensionless figure of merit ZT reaches 0.22 at 1000 K for the composition $(Ca_{0.995}Sr_{0.005})_3Co_4O_9$.

1. Introduction

The existence of a global warming due to greenhouse gas has now been largely demonstrated. Among greenhouse gas, the effect of CO_2 is preponderant, not because of a high greenhouse effect potential, which is in fact moderate, but due to the high amounts of CO_2 produced by various human activities (energy production, industrial activities, transports, ...). Consequently, reduction of CO_2 emissions in the atmosphere is required.

One of the most promising solutions to reduce CO_2 emissions is to use the waste heat to produce electricity through a thermoelectric device. Indeed, thermoelectric materials can convert exhaust heat energy directly into electrical energy without CO_2 emission. Nevertheless, thermoelectric generation is not widely used at present due to its low energy conversion efficiency η. The efficiency η is a function of the thermoelectric figure of merit $ZT = S^2\sigma T/\kappa$, where S is the Seebeck coefficient, σ is the electrical conductivity, T is the absolute temperature and κ is the thermal conductivity. As a result, the optimum material for thermoelectric generation should simultaneously exhibit large S, large σ and small κ.

The discovery of a large thermopower in the metallic oxide Na_xCoO_2 [1] has shown that oxides are potential candidates for thermoelectric applications. Due to their good stability they can be used as thermoelements working in oxidizing conditions up to 800 °C. However, because of the volatility of sodium at high temperature and hygroscopicity of Na_xCoO_2 in air, its application to power generation has been limited [2].

Nevertheless, other layered cobalt oxides have been shown to present excellent thermoelectric properties such as $Ca_3Co_4O_9$ [3]. This compound belongs to the family of misfit cobalt oxides [4–7]. Its crystal structure consists of CdI_2-type CoO_2 layers and triple rocksalt $[Ca_2CoO_3]$ layers stacking alternately along the c-axis. These two kind of layers have similar a, c, and β lattice parameters but different b parameter. To emphasize the incommensurate nature of the structure, $Ca_3Co_4O_9$ can be written as $[Ca_2CoO_3]_{(b2/b1)}[CoO_2]$, where $b1$ and $b2$ are two different lattice parameters for the rocksalt subsystem and the CoO_2 subsystem, respectively. The edge sharing CoO_2 octahedra layers are considered to be responsible for the electrical conduction, whereas the triple rocksalt layers can be regarded as a charge reservoir to supply charge carriers into the CoO_2 layers. However, if single crystals have shown ZT values close to 1 at 1000 K [3], polycrystalline ceramics present lower ZT values close to 0.1 at 1000 K [8] mainly due to their larger resistivity, which depends greatly on grain size, electrical properties of grain boundary, bulk density, and grain orientation. Many efforts have been made to improve the ZT values of polycrystalline ceramics of $Ca_3Co_4O_9$. For example, Matsubara et al. [9] have shown that increasing the grain alignment by Hot Pressing and Spark plasma Sintering treatments leads to increased ZT values. Horii et al. [10] have demonstrated that grain alignment by magnetic fields can allow doubling power factors, whereas Tani et al. [11] have synthesised the $Ca_3Co_4O_9$ phase using an in situ topotactic conversion of aligned platelet particles of $Co(OH)_2$ and reached a ZT value of 0.26 at 1055 K. However, if noticeable ZT improvements have been demonstrated by these grain orientation

* Corresponding author. Tel.: +33 1 64 69 70 82; fax: +33 1 64 69 75 55.
E-mail addresses: delormef@corning.com, fabiandelorme@yahoo.fr (F. Delorme).

0925-8388/$ – see front matter © 2010 Elsevier B.V. All rights reserved.
doi:10.1016/j.jallcom.2010.10.209

techniques, the ZT values are still far lower than ZT values of single crystals.

Another possibility to increase ZT values is the well-known addition of dopants and substitutions [12–16]. In the $Ca_3Co_4O_9$ compound, the substitution of Ca by Sr has been studied soon after the description of the phase structure. However, results are contradictory. According to Li et al. [17] the full substitution of Ca by Sr is possible, whereas Miyazaki et al. [18] have reported the apparition of a secondary phase ($(Sr,Ca)CoO_y$) since 30% substitution. Pelloquin et al. [19] have shown that to stabilize a "pure" $Sr_3Co_4O_9$ compound it is necessary to substitute 2% of cobalt in the rocksalt layers by small tetravalent elements such as Ti^{4+} or Ge^{4+}. Relative to the thermoelectric properties the reports are also contradictory. Some authors claim that the Sr substitution is detrimental to the thermoelectric properties of the compound: Li et al. [17] and Pelloquin et al. [19] have reported lower power factors when increasing the amount of Sr, Wang et al. [20] an increase of the resistivity as the Sr content increases, whereas Xia et al. [21] have reported a slight decrease of Seebeck coefficient. On the contrary, Miyazaki et al. [18] have reported for substitution up to 20%, a decrease in resistivity and Seebeck coefficient, leading to slightly higher power factors at 1000 K of 2, 2.1 and 2.3×10^{-4} W m^{-1} K^{-2} for 0, 10 and 20% Sr, respectively. Finally, Horii et al. [22], studying forged thick films, do not see any increase or decrease of the electrical conductivity, Seebeck coefficient or power factor up to 1100 K for Sr amounts varying from 5 to 20%. Moreover, Li et al. [17] have also noted that thermal conductivity at 700 °C is reduced from 1.7 for the pure $Ca_3Co_4O_9$ compound to 1.4 for the fully Sr substituted sample.

The aim of this paper is to study the influence of calcium substitution by strontium on the thermoelectric properties of the $Ca_3Co_4O_9$ compound.

2. Materials and methods

$Ca_3Co_4O_9$ samples were synthesised from $CaCO_3$ (Sigma–Aldrich, >99% purity), Co_3O_4 (Sigma–Aldrich) and $SrCO_3$ (Aldrich, 98+ % purity) as precursors. $(Ca_{1-x}Sr_x)_3Co_4O_9$ samples with $x = 0$, 0.001, 0.002, 0.004, 0.005, 0.006, 0.01, 0.02, 0.1, 0.2, 0.3, 0.5 and 1 have been realized. Stoichiometric amounts of the precursors were thoroughly mixed 5 min at 400 rpm in an agate ball mill (Retsch PM 100). The resulting black powder has been heated at 850 °C for 8 h at a rate of 5 °C/min, in an alumina crucible and slowly cooled down.

Sintering was performed by Spark Plasma Sintering (SPS, FCT Systeme GmbH HP D 25). The synthesised powders were placed in a 20 mm diameter graphite die. A pressure of 70 MPa was applied whereas the temperature was raised at 100 °C/min up to 850 °C for 5 min. Then the sample was cooled at 100 °C/min to room temperature. The obtained pellets were then polished to remove the graphite foils used during the SPS process and cut as bars for thermoelectric properties measurements or core drilled (12.7 mm diameter, 2 mm in thickness) for thermal conductivity measurements.

Thermoelectric properties of the sintered samples were determined from simultaneous measurement of resistivity and Seebeck coefficient in a ZEM III equipment (ULVAC Technologies) and thermal conductivity. The thermal conductivity, κ, was determined from thermal diffusivity, a, heat capacity, C_p, and density ρ, using the following equation: $\kappa = \rho\, a\, C_p$. The thermal diffusivity was measured using the laser flash diffusivity technique (Netzsch LFA 427) from room temperature to 800 °C in air atmosphere. The thermal diffusivity measurement of all specimens was carried out three times at each temperature. The heat capacity of the materials was measured from room temperature to 800 °C, with a heating rate of 10 °C min^{-1} in platinum crucibles and in air atmosphere, using differential scanning calorimetry (Netzsch DSC 404C pegasus).

Powder X-ray diffraction (XRD) patterns have been performed on a Philips X'PERT Pro θ/2θ diffractometer equipped with an X'CELERATOR real time multiple strip detector, using Cu-Kα radiation and operating at 45 kV and 40 mA at room temperature. The scans have been recorded from 5 to 140° (2θ) with a step of 0.00167° and a counting time of 40 s per step. The c-lattice parameter of the $(Ca_{1-x}Sr_x)_3Co_4O_9$ layered compound was calculated using the Rietveld refinement method employing the FullProf Suite program [23].

3. Results and discussion

Fig. 1a shows that after the synthesis process the unsubstituted sample ($x = 0$) is only composed by the $Ca_3Co_4O_9$ compound. Moreover, the SPS sintering process does not lead to the apparition of secondary phases (Fig. 1b).

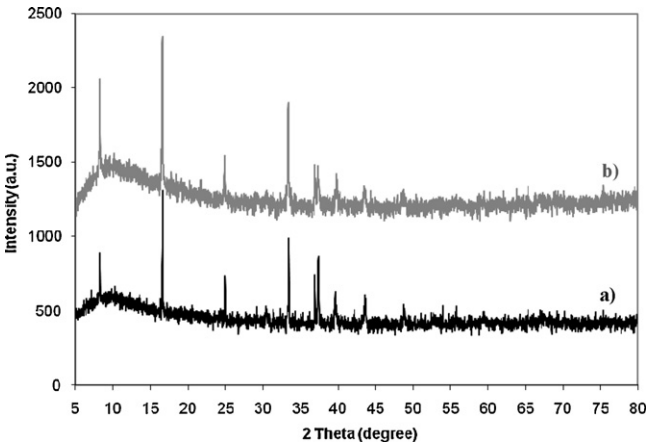

Fig. 1. Powder XRD patterns of $Ca_3Co_4O_9$ samples (a) before sintering and (b) after SPS sintering.

XRD patterns of the $(Ca_{1-x}Sr_x)_3Co_4O_9$ samples with $x = 0$, 0.01, 0.1, 0.3, 0.5 and 1 respectively, are shown in Fig. 2a–f. Samples with $x = 0$, 0.01 and 0.1 are single-phased presenting the $Ca_3Co_4O_9$ layered structure. For samples with $x = 0.3$ and 0.5, two phases are present, the $Ca_3Co_4O_9$ layered structure, which decreases when increasing Sr content and a non-layered structure which increases when increasing the Sr content. The $Sr_3Co_4O_9$ sample only presents the non-layered structure phase and small amounts of Co_3O_4. This non-layered structure phase corresponds to the $Sr_6Co_5O_{15}$ phase [24,25]. This phase belongs to a group of pseudo one-dimensional phases where the two end members are $Ca_3Co_2O_6$ and 2H-perovskite $BaCoO_{3-x}$ [26,27]. Thus, the composition of these phases can be written as $(A_3Co_2O_6)_m(A'_3Co_3O_9)_n$, where A and A′ are Ca, Sr or Ba. The $Sr_6Co_5O_{15}$ phase correspond to the $m = 1$ and $n = 1$ member of the family. $Ca_3Co_2O_6$ has Co–O chains in which CoO_6 octahedra and CoO_6 triangular prisms stack alternately by sharing their faces and calcium atoms isolate the Co–O chains, whereas in $Sr_6Co_5O_{15}$, one CoO_6 prism is stacked alternately with four consecutive CoO_6 octahedra blocks in the Co–O chains that are separated by strontium atoms.

Fig. 2a–d shows that the position of the peaks related to the layered structure of the $Ca_3Co_4O_9$ phase are shifting to lower

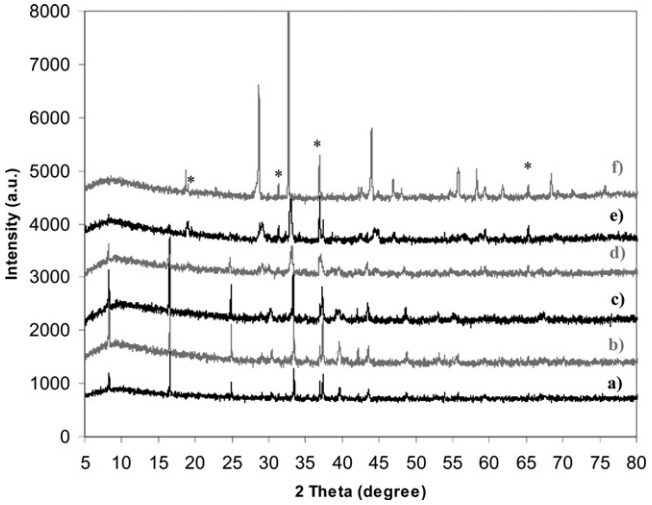

Fig. 2. Powder XRD patterns of the $(Ca_{1-x}Sr_x)_3Co_4O_9$ samples with a) $x = 0$, b) $x = 0.01$, c) $x = 0.1$, d) $x = 0.3$, e) $x = 0.5$ and f) $x = 1$. * is indicating the peaks corresponding to the Co_3O_4 compound.

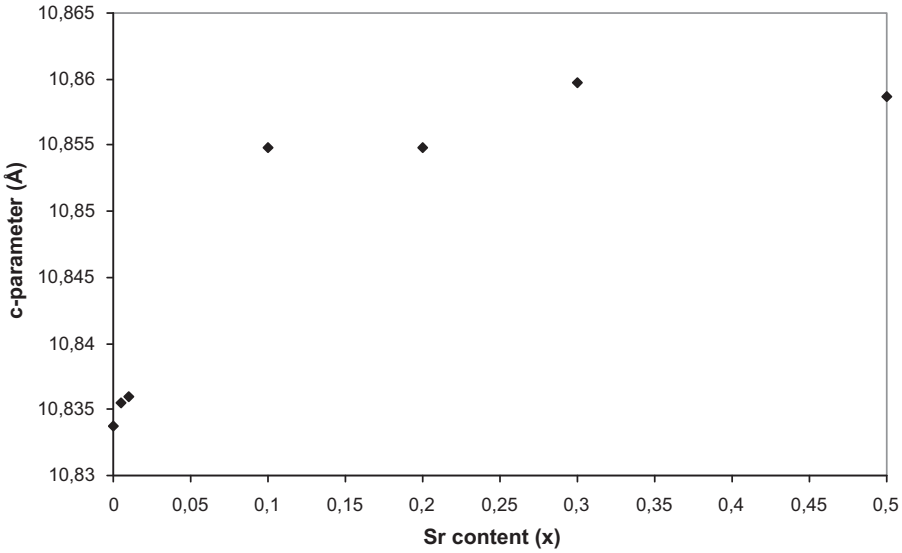

Fig. 3. Evolution of the c-parameter of the $(Ca_{1-x}Sr_x)_3Co_4O_9$ samples as a function of the Sr content.

2θ values as the Sr content increases. The *c*-parameter of the $(Ca_{1-x}Sr_x)_3Co_4O_9$ layered compounds increases with increasing the Sr content as shown in Fig. 3. This is consistent with a substitution of some calcium atoms (1.00 Å) by bigger strontium atoms (1.18 Å) [28]. Fig. 2d–f shows that $Sr_6Co_5O_{15}$ peak positions shift as the Sr content varies. In this case, this is consistent with a substitution of some strontium atoms (1.18 Å) by smaller calcium atoms (1.00 Å) [28].

All the sintered samples present a high bulk density with an apparent density value larger than 95% of the theoretical density.

Fig. 4 exhibits the temperature dependence of the Seebeck coefficient (S) of the $(Ca_{1-x}Sr_x)_3Co_4O_9$ samples with $x = 0$, 0.01, 0.1, 0.3 and 1 from 650 to 1000 K. The Seebeck coefficient of all the samples shows a positive value over the measured temperature range, indicating a p-type conduction. Fig. 4 clearly shows the difference of behaviour between samples with the bi-dimensional structure of $Ca_3Co_4O_9$ and samples with the pseudo one-dimensional structure of $Sr_6Co_5O_{15}$. Indeed, for the samples presenting the bi-dimensional structure of $Ca_3Co_4O_9$, the value of the Seebeck coefficient increases with increasing temperature, whereas for the sample presenting the pseudo one-dimensional structure of $Sr_6Co_5O_{15}$, the value of the Seebeck coefficient decreases as temperature increases. It appears that the substitution of Ca by Sr in the $Ca_3Co_4O_9$ structure does not lead to significant increase of the Seebeck coefficient (173 $\mu V K^{-1}$ at 1000 K). An increase of the Seebeck coefficient value can be observed for samples containing both the $Ca_3Co_4O_9$ structure and the $Sr_6Co_5O_{15}$ structures, especially at low temperature ($S = 164$ and 157 $\mu V K^{-1}$ at 650 K for $x = 0.3$ and $x = 0$ respectively). Finally the sample with $x = 1$, exhibits a different behaviour since S decreases as temperature increases from $S = 234\ \mu V K^{-1}$ at 650 K to $S = 182\ \mu V K^{-1}$ at 1000 K. The absence of variation of the Seebeck coefficient of samples with the $Ca_3Co_4O_9$ structure is consistent with the isovalent character of the substitution of Ca^{2+} by Sr^{2+} that does not affect the number of charge carriers.

The temperature dependence of the electrical conductivity (σ) of the $(Ca_{1-x}Sr_x)_3Co_4O_9$ samples with $x = 0$, 0.01, 0.1, 0.3 and 1 from 650 to 1000 K is shown in Fig. 5. All the samples exhibit the same behaviour whatever their structure, bi-dimensional or pseudo one-dimensional. The electrical conductivity increases with increasing temperature, which is characteristic of a semiconducting-like behaviour ($d\rho/dT \leq 0$). However, Fig. 5 shows three different behaviours. The samples presenting the pseudo one-dimensional structure of $Sr_6Co_5O_{15}$ ($x = 0.3$ and $x = 1$) exhibit significantly lower

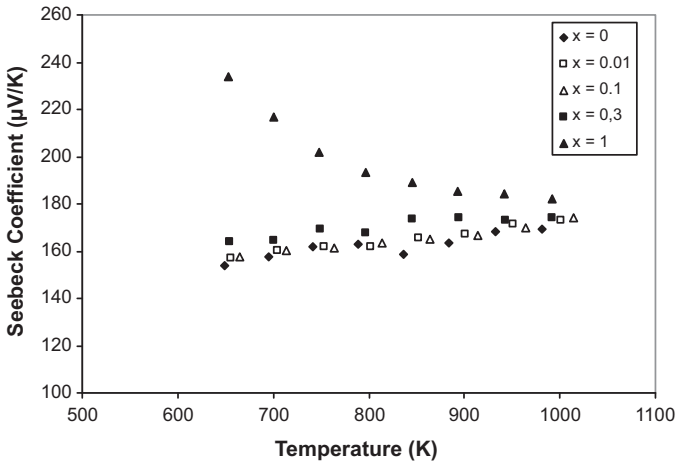

Fig. 4. Temperature dependence of the Seebeck coefficient of $(Ca_{1-x}Sr_x)_3Co_4O_9$ samples.

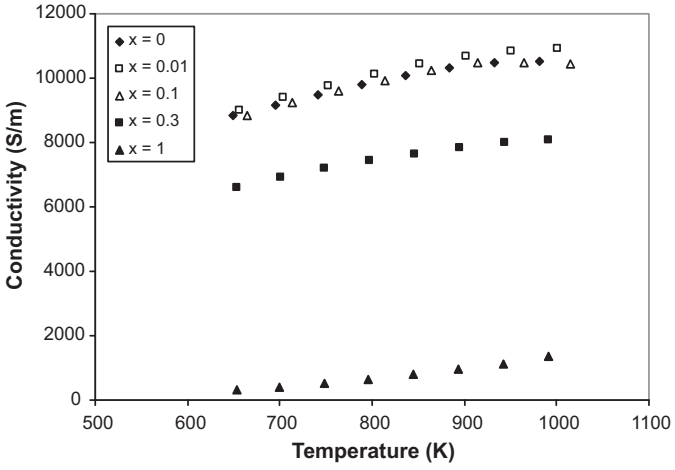

Fig. 5. Temperature dependence of the electrical conductivity of $(Ca_{1-x}Sr_x)_3Co_4O_9$ samples.

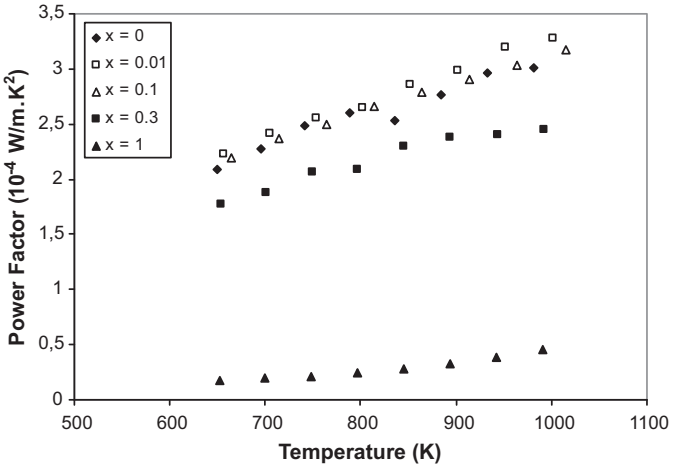

Fig. 6. Temperature dependence of the power factor of $(Ca_{1-x}Sr_x)_3Co_4O_9$ samples.

electrical conductivity values compared to the unsubstituted sample ($x = 0$), even for samples that are principally constituted by a $Ca_3Co_4O_9$ structure such as the sample with $x = 0.3$. At 1000 K, the electrical conductivity is 10500, 8089 and 1372 S m^{-1} for samples with $x = 0$, 0.3 and 1, respectively. The electrical conductivity of the sample with $x = 0.1$ is similar to the unsubstituted sample ($x = 0$). However for samples with low level of substitution ($x = 0.01$) the electrical conductivity is slightly higher, $\sigma = 10911$ S m^{-1} at 1000 K.

The temperature dependence of the power factor ($= S^2\sigma$) of the $(Ca_{1-x}Sr_x)_3Co_4O_9$ samples with $x = 0$, 0.01, 0.1, 0.3 and 1 from 650 to 1000 K is presented in Fig. 6. Three different behaviours can be observed as for the electrical conductivity. The samples presenting the pseudo one-dimensional structure of $Sr_6Co_5O_{15}$ ($x = 0.3$ and $x = 1$) exhibit significantly lower power factor values compared to the unsubstituted sample ($x = 0$), even for samples that are principally constituted by a $Ca_3Co_4O_9$ structure such the as sample with $x = 0.3$. At 1000 K, the power factor is 3.01, 2.45 and 0.45×10^{-4} W m^{-1} K^{-2} for samples with $x = 0$, 0.3 and 1, respectively. The power factor of the sample with $x = 0.1$ is similar to the unsubstituted sample ($x = 0$). However for samples with low level of substitution ($x = 0.01$) the power factor is slightly higher (3.25×10^{-4} W m^{-1} K^{-2} at 1000 K). Fig. 7a shows the evolution of the power factor value at 1000 K as a function of the Sr content of the samples from $x = 0$ to $x = 1$ and Fig. 7b is a detail of Fig. 7a from $x = 0$ to $x = 0.1$. These two figures clearly allow showing the three different behaviours. The first one is related to samples with the pseudo one-dimensional structure of $Sr_6Co_5O_{15}$ ($x \geq 0.3$) that exhibit lower power factors than the unsubstituted sample ($x = 0$). In this area the higher the Sr content, the lower the power factor. The second and third behaviours are related to samples presenting the bi-dimensional $Ca_3Co_4O_9$ structure. It appears that the Sr content does not significantly affect the power factor for most of the substitution rate in this area except for substitution rates close to 0.5% ($x = 0.005$). Indeed, a maximum power factor value (3.95×10^{-4} W m^{-1} K^{-2} at 1000 K) is obtained for samples containing 0.5% of Sr ($x = 0.005$). As already mentioned for the sample containing 1% of Sr ($x = 0.01$) and illustrated in Fig. 5, this high value is due to the highest electrical conductivity measured $\sigma = 12180$ S m^{-1} at 1000 K.

Temperature dependence of the thermal conductivity from 650 to 1000 K shows the same trend for all the $(Ca_{1-x}Sr_x)_3Co_4O_9$ samples. Indeed, thermal conductivity slightly decreases from room temperature to 1000 K, from 2.52 to 2.1 W m^{-1} K^{-1} for the unsubstituted sample ($x = 0$) and from 1.89 to 1.605 W m^{-1} K^{-1} for the sample with $x = 0.1$ for instance. This is consistent with the data already published concerning the $Ca_3Co_4O_9$ system [29,30]. The

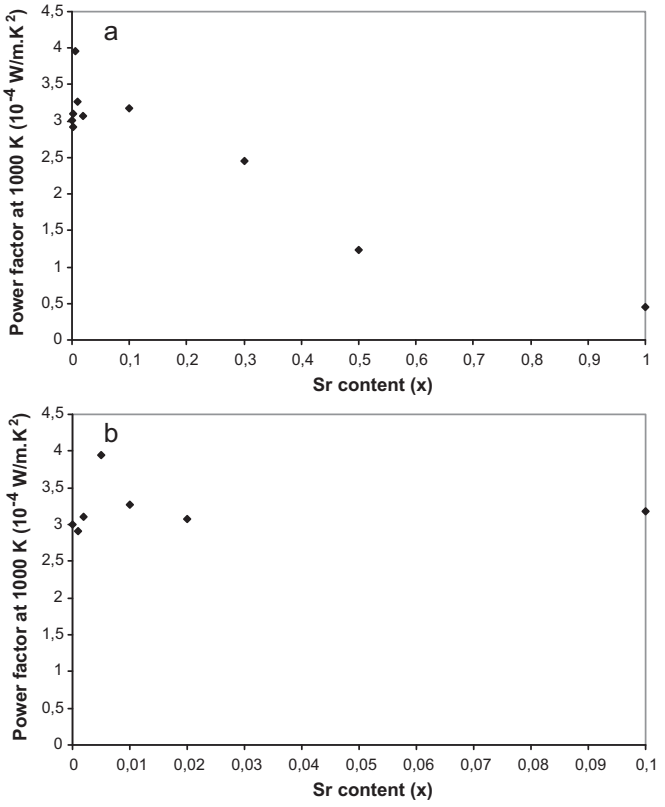

Fig. 7. (a) Evolution of the power factor value at 1000 K as a function of the Sr content, b) detail of 7a), from $x = 0$ to $x = 0.1$.

evolution of the thermal conductivity value at 1000 K as a function of the Sr content is plotted in Fig. 8. It clearly shows that even for the lowest substitution rates the thermal conductivity significantly decreases from 2.1 to 1.77 W m^{-1} K^{-1} for the unsubstituted sample ($x = 0$) and for the sample with $x = 0.005$, respectively. Moreover, the thermal conductivity value at 1000 K decreases linearly as the Sr content increases. Thermal conductivity can be expressed by the sum of lattice component (κ_l) and electronic component (κ_e) as $\kappa = \kappa_l + \kappa_e$. The κ_e values can be estimated from Wiedemann–Franz's law as $\kappa_e = LT\sigma$, where L is the Lorentz number (2.45×10^{-8} V^2 K^{-2} for free electrons). For the unsubstituted sample ($x = 0$) at 1000 K, $\kappa_e = 0.253$ W m^{-1} K^{-1}. As the electrical conductivity is in the same range for all the samples presenting the bi-dimensional $Ca_3Co_4O_9$ structure, that means that the thermal

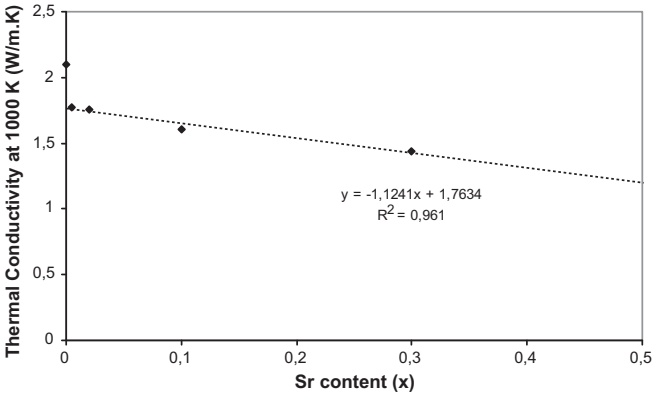

Fig. 8. Evolution of the thermal conductivity value at 1000 K as a function of the Sr content.

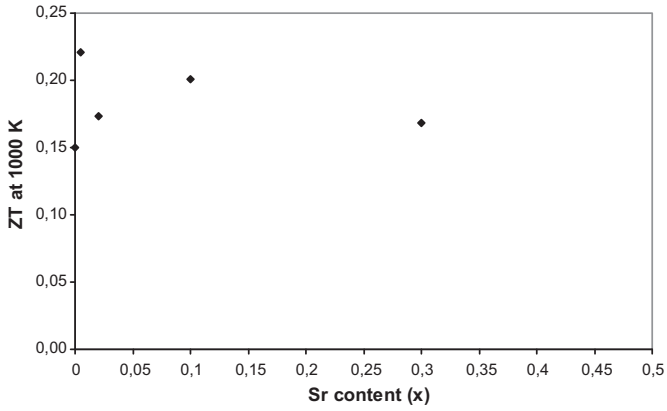

Fig. 9. Evolution of the ZT value at 1000 K as a function of the Sr content.

conductivity decrease observed when the Sr content increases, has to be related to the decrease of the lattice component of the thermal conductivity κ_l. This decrease has to be attributed to the increase of the phonon scattering due to the substitution of calcium atoms by heavier strontium atoms.

Finally, Fig. 9 shows the influence of the Sr content on the value at 1000 K of the dimensionless figure of merit ZT. It clearly shows that for all the samples containing Sr up to $x = 0.3$, the ZT value at 1000 K is higher than the ZT value of the unsubstituted sample ($x = 0$). The highest ZT value of 0.22 at 1000 K is exhibited by the sample with $x = 0.005$ compared to a ZT value of 0.15 for the $Ca_3Co_4O_9$ sample.

4. Conclusion

Sr substituted $(Ca_{1-x}Sr_x)_3Co_4O_9$ samples ($x = 0$, 0.001, 0.002, 0.004, 0.005, 0.006, 0.01, 0.02, 0.1, 0.2, 0.3, 0.5 and 1) have been prepared by solid state reaction, sintered by SPS and their thermoelectric properties at high temperature (650–1000 K) have been studied. XRD study has shown a structural change from a bi-dimensional $Ca_3Co_4O_9$-type compound to a pseudo one-dimensional phase of the type $Sr_6Co_5O_{15}$ when the Sr content increases. The $Sr_6Co_5O_{15}$-type phase appears for x values between 0.1 and 0.3, close to 0.2 according to XRD study. This means that for the considered thermal cycle the substitution limit of calcium by strontium is close to 0.2. The Ca–Sr substitution is well evidenced by the lattice parameter changes for both the bi-dimensional $Ca_3Co_4O_9$-type phase and the pseudo one-dimensional $Sr_6Co_5O_{15}$-type phase.

The effect of calcium substitution by strontium on the thermoelectric properties is complex. It confirms that the thermoelectric properties of materials with the pseudo one-dimensional $Sr_6Co_5O_{15}$-type structure are lower than those of materials with the bi-dimensional $Ca_3Co_4O_9$-type structure. Concerning materials with the bi-dimensional $Ca_3Co_4O_9$-type structure, the substitution of calcium by strontium does not significantly affect the Seebeck coefficient. However, an optimum value exists for 0.5% substitution in terms of electrical conductivity and power factor. Finally ZT values of samples containing up to 30% Sr ($x = 0.3$) increase due to the linear decrease of the thermal conductivities when the Sr content increases. The dimensionless figure of merit ZT reaches 0.22 at 1000K for the composition $(Ca_{0.995}Sr_{0.005})_3Co_4O_9$.

Acknowledgments

The authors would like to thank E. Francois, T. Montigny, G. Cadot, B. Deth and R. Olivon for the preparation of the samples.

References

[1] I. Terasaki, Y. Sasago, K. Uchinokura, Physical Review B 56 (1997) R12685–R12687.
[2] S. Li, R. Funahashi, I. Matsubara, K. Ueno, S. Sodeoka, H. Yamada, Journal of Materials Letters 19 (2000) 1339–1341.
[3] M. Shikano, R. Funahashi, Applied Physics Letters 82 (2003) 1851–1853.
[4] S. Li, R. Funahashi, I. Matsubara, K. Ueno, H. Yamada, Journal of Materials Chemistry 9 (1999) 1659–1660.
[5] A.C. Masset, C. Michel, A. Maignan, M. Hervieu, O. Toulemonde, F. Studer, B. Raveau, Physical Review B 62 (2000) 166–175.
[6] Y. Miyazaki, K. Kudo, M. Akoshima, Y. Ono, Y. Koike, T. Kajitani, Japanese Journal of Applied Physics 39 (2000) L531–L533.
[7] S. Lambert, H. Leligny, D. Grebille, Journal of Solid State Chemistry 160 (2001) 322–331.
[8] S. Li, R. Funahashi, I. Matsubara, K. Ueno, S. Sodeoka, H. Yamada, Chemistry of Materials 12 (2000) 2424–2427.
[9] I. Matsubara, R. Funahashi, T. Takeuchi, Y. Zhou, Preparation and thermoelectric properties of grain aligned $(Ca,Bi)_3Co_4O_9$ ceramics, in: 20th International Conference on Thermoelectrics, 2001, pp. 172–175.
[10] S. Horii, I. Matsubara, M. Sano, K. Fujie, M. Suzuki, R. Funahashi, M. Shikano, W. Shin, N. Murayama, J.-I. Shimoyama, K. Kishio, Japanese Journal of Applied Physics 42 (2003) 7018–7022.
[11] T. Tani, H. Itahara, C. Xia, J. Sugiyama, Journal of Materials Chemistry 13 (2003) 1865–1867.
[12] V.A.M. Brabers, H. Meuter, Z. Simsa, Solid State Communications 45 (1983) 807–809.
[13] T. Tsubota, M. Ohtaki, K. Eguchi, H. Arai, Journal of Materials Chemistry 7 (1997) 85–90.
[14] M. Ohtaki, T. Tsubota, K. Eguchi, Thermoelectric properties of oxide solid solutions based on Al-doped ZnO, in: 17th International Conference on Thermoelectrics, 1998, pp. 610–613.
[15] W. Shin, N. Murayama, Japanese Journal of Applied Physics 38 (1999) L1336–L1338.
[16] J.-W. Moon, W.-S. Seo, H. Okabe, T. Okawa, K. Koumoto, Journal of Materials Chemistry 10 (2000) 2007–2009.
[17] S. Li, R. Funahashi, I. Matsubara, H. Yamada, K. Ueno, S. Sodeoka, Ceramics International 27 (2001) 321–324.
[18] Y. Miyazaki, T. Miura, Y. Ono, T. Mashi, T. Goto, T. Kajitani, Crystal structure and thermoelectric properties of the composite crystal $[(Ca_{1-x}Sr_x)_2CoO_3]_pCoO_2$, in: 21st International Conference on Thermoelectronics, 2002, pp. 226–229.
[19] D. Pelloquin, S. Hebert, A. Maignan, B. Raveau, Solid State Sciences 6 (2004) 167–172.
[20] L.B. Wang, A. Maignan, D. Pelloquin, S. Hebert, B. Raveau, Journal of Applied Physics 92 (2002) 124–128.
[21] C. Xia, J. Sugiyama, H. Itahara, T. Tani, Journal of Crystal Growth 276 (2005) 519–524.
[22] S. Horii, Y. Yamasaki, M. Sakurai, R. Funahashi, T. Uchikoshi, T.S. Suzuki, Y. Sakka, H. Ogino, J.-I. Shimoyama, K. Kishio, Materials Research Society Symposium Proceedings 1044 (2008) U03–U09.
[23] J. Rodriguez-Carvajal, Commission on Powder Diffraction (IUCr) Newsletter 26 (2001) 12–19.
[24] W.T.A. Harrison, S.L. Hegwood, A.J. Jacobson, Journal of the Chemical Society-Chemical Communications (1995) 1953–1954.
[25] K. Iwasaki, M. Shimada, H. Yamane, J. Takahashi, S. Kubota, T. Nagasaki, Y. Arita, J. Yuhara, Y. Nishi, T. Matsui, Journal of Alloys and Compounds 377 (2004) 272–276.
[26] J.M. Perez-Mato, M. Zakhour-Nakhl, F. Weill, J. Darriet, Journal of Materials Chemistry 9 (1999) 2795–2808.
[27] K. Boulahya, M. Parras, J.M. Gonzalez-Calbet, Chemistry of Materials 12 (2000) 25–32.
[28] R.D. Shannon, Acta Crystallographica Section A 32 (1976) 751–767.
[29] D. Wang, L. Chen, Q. Wang, J. Li, Journal of Alloys and Compounds 376 (2004) 58–61.
[30] D. Wang, L. Chen, Q. Yao, J. Li, Solid State Communications 129 (2004) 615–618.